Journal of Solid State Chemistry **160,** 156–166 (2001)
doi:10.1006/jssc.2001.9210, available online at http://www.idealibrary.com on IDEAL®

New Ternary Phases in the Mo–Ni–P System: Synthesis and Crystal Structures

S. V. Oryshchyn,*,† C. Le Sénéchal,* S. Députier,* J. Bauer,* R. Guérin,* and L. G. Akselrud†

*Laboratoire de Chimie du Solide et Inorganique Moléculaire, UMR CNRS 6511, CNRS–Université de Rennes 1, Institut de Chimie, Campus de Beaulieu, Avenue du Général Leclerc, 35042 Rennes Cédex, France; and †Analytical Chemistry Department, Ivan Franko State University, Kyrylo and Mefodij Street 6, 290005 L'viv, Ukraine

E-mail: roland.guerin@univ-rennes1.fr

Received December 16, 2000; in revised form March 29, 2001; accepted April 12, 2001; published online June 12, 2001

A reinvestigation of the ternary system Mo–Ni–P has been established using X-ray diffraction, scanning electron microscopy, and electron probe microanalysis. This up-to-date system shows 10 ternary phosphides, which were mostly structurally characterized from X-ray powder or single-crystal data. Among these phosphides, three new ternary phases are reported for the first time: triclinic $Mo_{8.58}Ni_{7.42}P_6$ ($a = 7.0079(4)$ Å, $b = 7.0290(4)$ Å, $c = 7.0308(4)$ Å, $\alpha = 68.893(3)^\circ$, $\beta = 73.196(3)^\circ$, $\gamma = 60.149(3)^\circ$, space group $P\bar{1}$, new structure type), cubic $Mo_3Ni_2P_{1.18}$ ($a = 10.846(2)$ Å, space group $F\bar{4}3m$, Mn_3Ni_2Si-type structure), and tetragonal $Mo_{2.675}Ni_{0.325}P$ ($a = 9.733(1)$ Å, $b = 4.7805(7)$ Å, space group $I\bar{4}$, Mo_3P-type derivative structure). These phases were prepared from the elements by high-temperature annealing at 1350°C, and their crystal structures exhibit numerous strong metal–metal bonds in agreement with their metal-to-nonmetal ratio higher than 2.5. Indeed, in a general way, the phosphorus coordination number for Mo and Ni atoms is relatively small so that metallic arrangements as $[Ni_4]$ tetrahedra and $[Mo_6]$ octahedra can be considered as examples in the structures of $Mo_{8.58}Ni_{7.42}P_6$ and $Mo_3Ni_2P_{1.18}$, respectively. © 2001 Academic Press

Key Words: **molybdenum nickel phosphides; crystal data; structural relationship; electron probe microanalysis.**

INTRODUCTION

The first results on the ternary Mo–Ni–P system were obtained at the end of the 1970's when the composition lines NiP–MoP and Ni_2P–"Mo_2P" were studied at 1000°C by Guérin and Sergent (1, 2). Two ternary phases, namely $MoNiP_2$ and MoNiP, with hexagonal symmetry, were discovered at that time. The first one, a new structural type, exhibited strong linear and infinite –Mo–Ni–Mo– chains (3), whereas the second one, MoNiP, was found to be in fact the Mo-rich limit of a solid solution $Ni_{2-x}Mo_xP$ ($0 \leq x \leq 1$) of Fe_2P type (4).

Approximately at the same time, Oryshchyn *et al.* established at 850°C the isothermal section of the Mo–Ni–P phase diagram by means of X-ray analysis (5). In addition to the phases mentioned above, five new phosphides were isolated and labeled from I to V: I–Mo_2Ni_3P, II ~ $Mo_3Ni_7P_3$, III–$Mo_2Ni_6P_3$, IV ~ $Mo_3Ni_3P_2$, and V ~ Mo_2NiP. In a second step, the crystal structures of I–Mo_2Ni_3P and III–$Mo_2Ni_6P_3$ were solved by X-ray powder and single-crystal determination, respectively (5, 6). In contrast, in the absence of single crystals or pure samples, no crystallographic data for the last three phases II ~ $Mo_3Ni_7P_3$, IV ~ $Mo_3Ni_3P_2$, and V ~ Mo_2NiP could be obtained.

The goal of this study was therefore to synthesize at higher temperature the last three phosphides in order to obtain single crystals suitable for their structure determination. This paper deals with the results that were obtained after successive anneals of the samples at 1150 and 1350°C, using X-ray diffraction (XRD), scanning electron microscopy (SEM), and electron probe microanalysis (EPMA). In addition, for the first time the crystal structures of the new ternary phases $Mo_{8.58}Ni_{7.42}P_6$, $Mo_3Ni_2P_{1.18}$, and $Mo_{2.675}Ni_{0.325}P$ are described.

EXPERIMENTAL

Sample Preparation

The samples were prepared either as powders or as single crystals. The required amounts of the constituent elements, all as powders (Mo and Ni, purity 99.9%; and red phosphorus, purity 99.99%) were mixed, cold-pressed as pellets, and first annealed at 1000°C for two days in vacuum-sealed silica tubes. After cooling, samples were ground to powder, cold-pressed again, and reannealed at 1150°C under the same conditions for one week. After quenching, they were pulverized for X-ray powder diffraction.

To obtain single crystals, a second step was necessary. The previous samples were cold-pressed again and loaded

0022-4596/01 $35.00

into alumina crucibles, inside molybdenum containers (both crucibles were previously cleaned, by heating at 1500°C for 15 min under a dynamic vacuum of about 10^{-5} Torr). The Mo containers were then sealed under a low argon pressure using an arc-welding system. The charges were heated at a rate of 300°C/h up to 1350°C and maintained at this temperature for 8 h. They were then cooled in several steps (rate of 5°C/h down to 1100°C, then 10°C/h to 900°C, and finally furnace cooled). By this way, all samples were melted and showed metallic luster.

Powder Diffraction and Microprobe Analysis

The samples were then cut into three pieces. One part was pulverized and analyzed using X-ray powder diffraction (CPS 120 INEL) (monochromated Cu$K\alpha_1$ radiation, $\lambda = 1.54056$ Å) equipped with a position-sensitive detector covering 120° in 2θ (elemental silicon was taken to determine a cubic spline calibration function to describe the 2θ vs channel number calibration). A second part was kept for research of single crystals in the molten matrix. The last part was embedded in epoxy resin and polished down to 0.25 mm diamond grade, in order to obtain a perfect plane surface. The samples were then coated with either a gold or graphite thin layer to obtain good surface conductivity. Backscattered electron images were performed with a Jeol JSM-6400 SEM. Composition analysis was done in order to determine accurate phase compositions, possible inhomogeneities, and additional impurity phases. This analysis was first carried out by energy-dispersive spectroscopy of X-rays (GaP, Ni, and Mo metal as standards) and confirmed further with a Camebax SX 50 electron microprobe using wavelength-dispersive spectroscopy (WDS) of X-rays (InP, Mo metal, Ni metal, and/or NiO as standards). EPMA measurements were found to be in good agreement with phase compositions observed by powder diffraction and empirical formulas deduced from single-crystal data refinement.

TABLE 1
Crystal Data, Intensity Collection, and Refinement for $Mo_{8.58}Ni_{7.42}P_6$ and $Mo_3Ni_2P_{1.18}$

Empirical formula	$Mo_{8.58}Ni_{7.42}P_6$	$Mo_3Ni_2P_{1.18}$
Formula weight ($g.mol^{-1}$)	1444.61	441.78
Crystal system	Triclinic	Cubic
Space group	$P\bar{1}$	$F\bar{4}3m$
a (Å)	7.0079(4)	10.846(2)
b (Å)	7.0290(4)	
c (Å)	7.0308(4)	
α(°)	68.893(3)	
β(°)	73.196(3)	
γ(°)	60.149(3)	
V (Å^3)	277.63(7)	1275.9(5)
Z; calculated density ($g.cm^{-3}$)	1; 8.640(2)	16; 9.190(4)
Crystal size (mm^3)	$0.045 \times 0.045 \times 0.19$	$0.03 \times 0.03 \times 0.012$
Linear absorption coefficient (mm^{-1})	22.07	23.01
Refinement limits		
θ (°)	1–35	1–40
h, k, l	$0 < h < 10$; $-9 < k < 10$; $-10 < l < 11$	$0 < h < 19$; $0 < k < 13$; $0 < l < 12$
Reflections collected	3217	2358
Independent reflections (R_{int})	3056 (0.10)	1486 (0.059)
Reflections in refinement ($I > 4\sigma(I)$)	1937	246
Variable parameters	104	20
Absorption correction (T_{min}, T_{max})	0.075, 0.370	0.118, 0.307
Refinement	F	F
R	0.043	0.032
R_w with $w = 1/[\sigma(F_o^2) + (pF_o^2)]$	0.055 (p = 0.0045)	0.038 (p = 0.0020)
Extinction coefficient (Sheldrick)	$4.0(5) \times 10^{-3}$	$3.1(5) \times 10^{-4}$
Scale factor	0.727(2)	0.610(4)
Goodness-of-fit	1.030	0.990
Max. diff. peak ($e^-/Å^3$)	1.8	1.6

Single-Crystal X-Ray Diffraction

Single crystals of $Mo_{8.58}Ni_{7.42}P_6$, $Mo_3Ni_2P_{1.18}$, and $Mo_{2.675}Ni_{0.325}P$ could be extracted from molten samples. The intensity data collection was carried out at ambient temperature, using a Nonius KappaCCD X-ray area-detector diffractometer using Mo$K\alpha$ radiation ($\lambda = 0.71073$ Å). Data collection strategy was performed with the help of the COLLECT program (7) and reflections were corrected from Lorentz factors and polarization effects by the DENZO program of the KappaCCD software package (8). Absorption correction, taking into account the crystal morphology, was applied with the SORTAV program (9). Structures were solved by direct methods (program CSD97 (10) or SIR97 (11)). Least-squares refinements and difference Fourier syntheses were performed either with the CSD program package (10) for $Mo_{8.58}Ni_{7.42}P_6$ and $Mo_3Ni_2P_{1.18}$ or the beta version of JANA2000 (12) for $Mo_{2.675}Ni_{0.325}P$. Crystal structure and refinement data are given in Tables 1 and 7. The 3D structure representations of $Mo_{8.58}Ni_{7.42}P_6$ and $Mo_3Ni_2P_{1.18}$ were done using the DIAMOND program (13).

RESULTS AND DISCUSSION

Ternary Phase Diagram

The isothermal section of the phase diagram Mo–Ni–P at 850°C, reported in 1981 by Oryshchyn *et al.* (5), is given in Fig. 1. In addition to the extended solid solution

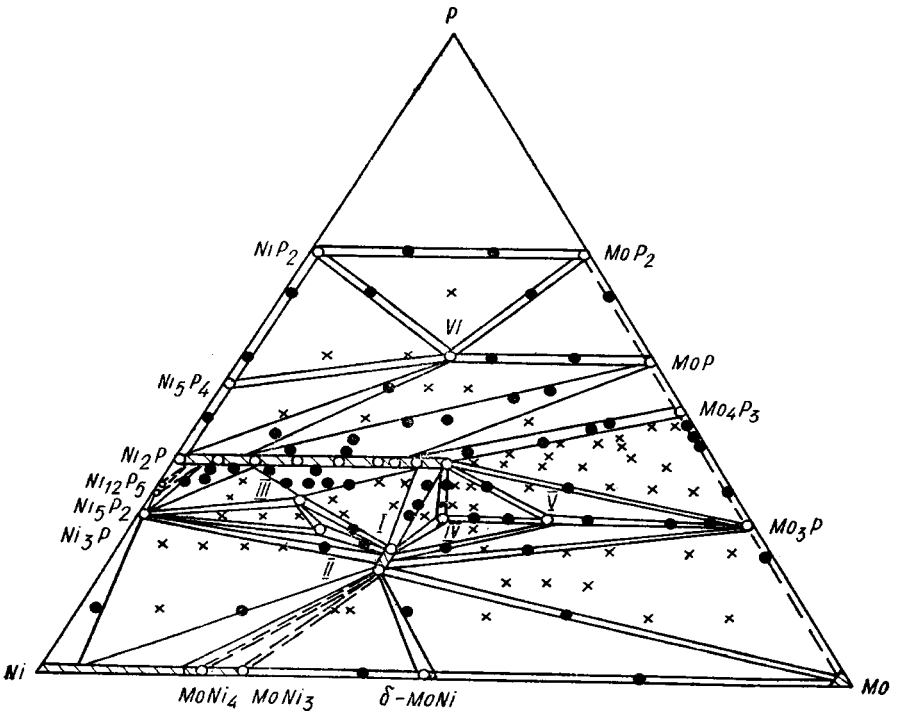

FIG. 1. Isothermal section of the Mo–Ni–P phase diagram at 850°C: The labeling of the ternary phases is as follows: I–Mo_2Ni_3P, II ~ $Mo_3Ni_7P_3$, III–$Mo_2Ni_6P_3$, IV ~ $Mo_3Ni_3P_2$, and V ~ Mo_2NiP, VI–$MoNiP_2$. ○, 1-phase range; ●, 2-phase range; ×, 3-phase range.

$Ni_{2-x}Mo_xP$ ($0 \leq x \leq 1$) of Fe_2P type (4, 14) and the ternary $MoNiP_2$ (hexagonal, space group $P6_3/mmc$, new structure type) (3) previously reported, five new phases labeled from I to V were mentioned at that time, with nominal compositions I–Mo_2Ni_3P, II ~ $Mo_3Ni_7P_3$, III–$Mo_2Ni_6P_3$, IV ~ $Mo_3Ni_3P_2$, and V ~ Mo_2NiP. The crystal structures of I–Mo_2Ni_3P (hexagonal, $P6_3/mmc$, disordered $MgZn_2$-type structure) (5) and III–$Mo_2Ni_6P_3$ (orthorhombic, $Pmmn$, new structure type) (6) were subsequently solved from X-ray powder and single-crystal data, respectively. In contrast, no crystallographic data for characterizing the other three ternary compounds II ~ $Mo_3Ni_7P_3$, IV ~ $Mo_3Ni_3P_2$, and V ~ Mo_2NiP could be obtained at the time.

The first step of our work was therefore to prepare these phases again in order to obtain single crystals for their structure determination. The high-temperature annealing of nominal compositions, first at 1150°C, then at 1350°C, led to molten samples corresponding to mixtures, as observed by X-ray diffraction and backscattered electron images coupled to EPMA. Thereby, in addition to the binary compound Ni_3P, six ternary phosphides could be identified with the following chemical formulas (average atomic proportions by EPMA given in parentheses; standard deviations estimated less than 1 at. %): $Mo_9Ni_6P_5$ (Mo:Ni:P = 45.05:29.40:25.55), $Mo_{2.65}Ni_{0.35}P$ (66.30:7.85:25.85), $Mo_{8.5}Ni_{7.5}P_6$ (38.40:33.35:28.25), Mo_3Ni_2P (49.80:33.70:16.50), $MoNi_2P$ (22.35:51.75:25.90), and Mo_2Ni_3P (32.60:51.10:16.30). Four of these phosphides were previously reported but with slightly modified atomic compositions (5). Indeed, if the ternary Mo_2Ni_3P is truly the phase I of $MgZn_2$-type structure, the phosphides $MoNi_2P$, $Mo_{8.5}Ni_{7.5}P_6$, and $Mo_9Ni_6P_5$ correspond to the phases previously labeled II ~ $Mo_3Ni_7P_3$, IV ~ $Mo_3Ni_3P_2$, and V ~ Mo_2NiP, respectively. At last, two new phases were evidenced: the first one seems to correspond to the Ni-rich limit of a substitution solid solution $Mo_{3-x}Ni_xP$ ($0 \leq x \leq 0.35$), whereas the second one appears as a ternary compound Mo_3Ni_2P, probably a high-temperature phase, since it was present in all the three samples synthesized at 1350°C but was not observed at 850°C.

Needle-shaped single crystals of the three ternary phases $Mo_{8.5}Ni_{7.5}P_6$, Mo_3Ni_2P, and $Mo_{3-x}Ni_xP$ ($x \sim 0.35$) could be extracted from molten samples and used for structure determination. Unfortunately, numerous attempts to synthesize at different temperatures the last two phases $Mo_9Ni_6P_5$ and $MoNi_2P$, either as single crystals or as pure samples, have been unsuccessful so far. Indeed, in the absence of single crystals, the X-ray powder patterns are much too complicated to access the crystallographic data. As shown in Fig. 2a, the SEM diagram of a molten sample with nominal composition $Mo_9Ni_6P_5$ shows a mixture of three phases, $Mo_{3-x}Ni_xP$ ($x \sim 0.35$), Mo_2Ni_3P, and $Mo_9Ni_6P_5$ itself, while the diagram of $MoNi_2P$ exhibits several phases

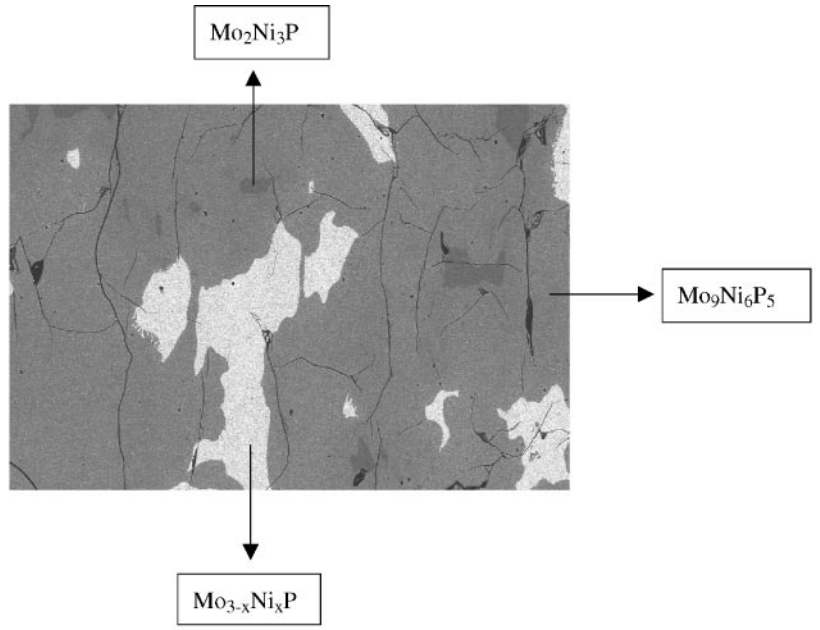

(a)

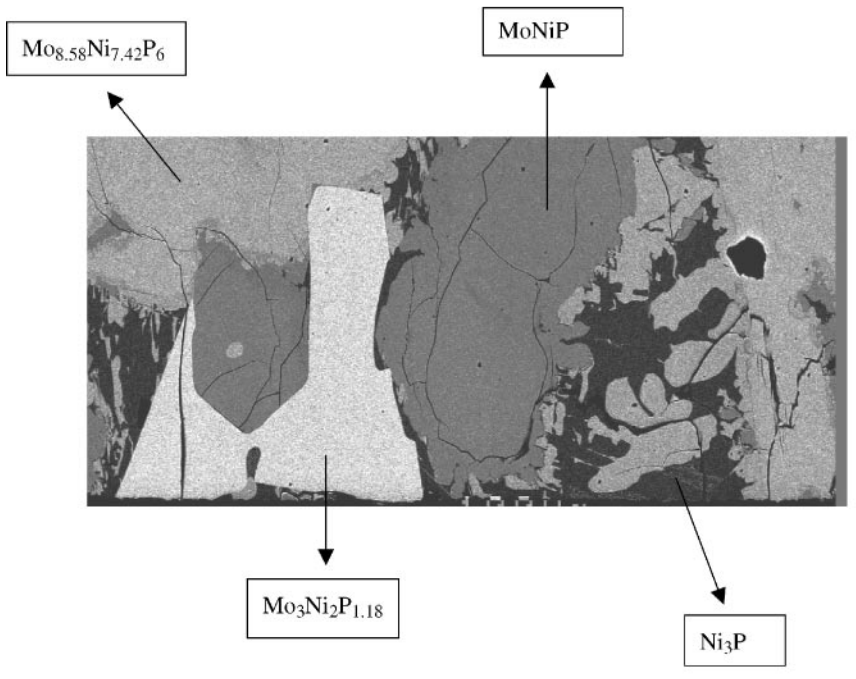

(b)

FIG. 2. SEM diagram of molten samples synthesized at 1350°C: (a) $Mo_9Ni_6P_5$ and (b) $MoNi_2P$.

such as Ni_3P, Mo_3Ni_2P, $Mo_{8.5}Ni_{7.5}P_6$, and MoNiP (Fig. 2b).

Finally, the study at 1350°C confirms for a large part previous results obtained at 850°C by means of X-ray diffraction only. Nevertheless, by combining SEM and EPMA with X-rays, a more precise composition of some phases, not yet structurally described, was found. The only significant difference between studies at 850° and those at 1350°C results from the occurrence of two new phases, Mo_3Ni_2P and $Mo_{3-x}Ni_xP$ ($x \sim 0.35$), by high-temperature synthesis. Table 2 summarizes the main crystallographic data of the phases belonging to the Mo–Ni–P system. It can be noted

TABLE 2
Crystallographic Data of the Ternary Phases in the Mo–Ni–P System

Compound	*a* (Å)	*b* (Å)	*c* (Å)	Space group
I–Mo_2Ni_3P	4.688(2)		7.601(4)	$P6_3/mmc$
III–$Mo_2Ni_6P_3$	12.94(2)	3.568(5)	5.911(5)	$Pmmn$
[a]IV–$Mo_{8.58}Ni_{7.42}P_6$	7.0079(4)	7.0290(4)	7.0308(4)	$P\bar{1}$
	$\alpha = 68.893(3)$	$\beta = 73.196(3)$	$\gamma = 60.149(3)$	
VI–$MoNiP_2$	3.329(3)		11.22(1)	$P6_3/mmc$
[b]MoNiP	5.861(3)		3.704(2)	$P\bar{6}2m$
[a]$Mo_3Ni_2P_{1.18}$	10.846(2)			$F\bar{4}3m$
[a]$Mo_{2.675}Ni_{0.325}P$	9.733(1)		4.7805(7)	$I\bar{4}$
$MoNiP_8$	6.235(2)		8.747(3)	$P\bar{3}1c$

Note. Labeling of phases is that used in the ternary Mo–Ni–P phase diagram (Fig. 1); for the phases II ~ $Mo_3Ni_7P_3$ and V ~ Mo_2NiP, see text.
[a]Phases structurally studied during this work.
[b]Ni-rich limit of the $Ni_{2-x}Mo_xP$ solid solution ($0 \le x \le 1$).

that this table includes a phosphorus-rich compound $MoNiP_8$, prepared 10 years ago by the tin flux method (15).

Crystal Structure Description

The crystal structures of the ternary compounds $Mo_{8.5}Ni_{7.5}P_6$, Mo_3Ni_2P, and $Mo_{3-x}Ni_xP$ ($x \sim 0.35$) were solved on single crystals. About 20 crystals were tested for the first two phases in order to choose the best candidates for intensity data collection. The problem was somewhat different for the $Mo_{3-x}Ni_xP$ phase, since only two single crystals of good quality could be isolated from the different molten samples.

1. $Mo_{8.58}Ni_{7.42}P_6$. Crystal data and further details of the data collection are given in Table 1. The structure of $Mo_{8.58}Ni_{7.42}P_6$ was solved in the centrosymmetric space group $P\bar{1}$. The application of direct methods revealed that all atoms occupy the general position (2i), with the exception of one nickel atom Ni3 in the (1f) position and one atom, initially named Mo5, in the (1a) position. All positions were subsequently refined with isotropic thermal parameters. Due to an unreasonable thermal parameter for the atom Mo5, a mixed Mo/Ni position (58 at.% Mo, 42 at.% Ni) was proposed and refined on the (1a) position, yielding reasonable isotropic thermal parameters. The reliability factors were improved when anisotropic thermal parameters were refined together with a secondary extinction factor. At the end of refinement, the equivalent isotropic thermal parameters were found to be less than 0.60 Å^2. The residual values R and R_w (0.043 and 0.055, respectively) were obtained for 104 variable parameters and 1937 structure factors with $I > 4\sigma(I)$. A final difference Fourier synthesis did not reveal any significant electron density peaks. The formula of this phosphide, deduced from structure refinement, is therefore $Mo_{8.58}Ni_{7.42}P_6$, leading to the atomic proportions Mo:Ni:P = 39.00:33.73:27.27. This result fits nicely with the nominal overall composition by EPMA (38.40:33.35:28.25). Atomic positional, thermal coordinates and selected interatomic distances are given in Tables 3 and 4, respectively.

The 3D representation of the structure (Fig. 3a) shows a relatively simple atomic arrangement, which favors the occurrence of numerous and strong metal-metal bonds, in agreement with the metal-to-nonmetal ratio of 2.66. Indeed, with the exception of the (Mo, Ni)5 atom surrounded by six phosphorus atoms, the other metal atoms exhibit quite small phosphorus coordination numbers (4 for Mo1 to Mo4, 2 for Ni1 to Ni3, 3 for Ni4). The main characteristics of the structure can be viewed especially from Ni–Ni bonds since Ni atoms are displayed per unit cell in two tetrahedral-like [Ni_4] clusters, one up and one down, with a common edge (all Ni–Ni distances comprise between 2.621 and 2.757 Å). These groups of two tetrahedra are connected to each other, by means of the isolated Ni3 atoms (2.600 and 2.605 Å), in such a way that infinite chains of nickel atoms are generated, along the [010] direction (Fig. 3b). Other infinite chains of edge-shared tetrahedral [Ni_4] clusters in ternary phosphides such as $Ni_4Nb_5P_4$, $SmNi_4P_2$, and $ZrNi_4P_2$ were recently described in the literature (16).

2. $Mo_3Ni_2P_{1.18}$. Identification of this compound leads to the following type of crystal lattice: cubic unit cell, 16 formulas per unit cell, Laüe group $m3m$, space group $F\bar{4}3m$ in agreement with systematic absences of the reflections hkl ($h + k, k + l, h + l \neq 2n$) and hhl ($h + l \neq 2n$). The crystal data, intensity collection, and refinement conditions are given in Table 1. The application of direct methods first gave five independent atom positions corresponding to 48

TABLE 3
Atomic Positional and Thermal Coordinates for $Mo_{8.58}Ni_{7.42}P_6$

Atom	Position	*x*	*y*	*z*	[a]$B_{eq.}$ (Å^2)
Mo1	2(i)	0.30077(8)	0.05341(8)	0.16108(7)	0.49(1)
Mo2	2(i)	0.92662(8)	0.46458(8)	0.84945(7)	0.55(1)
Mo3	2(i)	0.56330(8)	0.28417(8)	0.14281(8)	0.57(1)
Mo4	2(i)	0.05938(8)	0.13099(8)	0.56258(8)	0.54(1)
[b]Mo5	1(a)	0	0	0	0.58(2)
Ni1	2(i)	0.6319(1)	0.2868(1)	0.4989(1)	0.49(2)
Ni2	2(i)	0.2174(1)	0.4197(1)	0.4971(1)	0.54(2)
Ni3	1(f)	1/2	0	1/2	0.53(3)
Ni4	2(i)	0.3562(1)	0.3800(1)	0.8317(1)	0.42(2)
P1	2(i)	0.7006(2)	0.3320(2)	0.7711(2)	0.46(4)
P2	2(i)	0.9018(2)	0.2644(2)	0.2332(2)	0.44(4)
P3	2(i)	0.2961(2)	0.1246(2)	0.7812(2)	0.44(4)

[a]$B_{eq} = 1/3[B_{11}\, a^{*2}\, a^2 + \ldots 2B_{23}\, b^*\, c^*\, b\, c \cos(\alpha)]$.
[b]A mixed Mo/Ni position: 58.2(6) at.% Mo and 41.8(6) at.% Ni.

TABLE 4
Main Interatomic Distances (Å) of $Mo_{8.58}Ni_{7.42}P_6$ (< 3.30 Å)

Mo1	1P2	2.423(2)	Mo4–	1Ni1	2.746(1)	Ni4–	1P1	2.196(2)
	1P3	2.541(2)		1Mo4	2.824(1)		1P3	2.197(2)
	1P3	2.547(2)		1Mo5	2.843(1)		1P2	2.209(2)
	1P1	2.580(2)		1Mo1	2.925(1)		1Ni1	2.621(1)
	1Ni1	2.659(1)		1Mo1	3.230(1)		1Ni1	2.656(1)
	1Ni4	2.706(1)		1Mo2	3.253(1)		1Ni2	2.672(1)
	1Ni4	2.781(1)		1Mo2	3.266(1)		1Mo3	2.673(1)
	1Mo5	2.888(1)					1Mo2	2.680(1)
	1Ni3	2.920(1)	Mo5–	2P3	2.536(2)		1Mo1	2.706(1)
	1Mo2	2.922(1)		2P1	2.610(2)		1Mo2	2.736(1)
	1Mo4	2.925(1)		2P2	2.624(2)		1Mo3	2.759(1)
	1Mo3	2.952(1)		2Mo3	2.819(1)		1Mo1	2.781(1)
	1Mo1	2.996(1)		2Mo4	2.843(1)			
	1Mo4	3.230(1)		2Mo2	2.864(1)	P1–	1Ni4	2.196(2)
				2Mo1	2.888(1)		1Ni2	2.221(2)
Mo2–	1P1	2.454(2)					1Ni1	2.262(2)
	1P2	2.548(2)	Ni1–	1P2	2.228(2)		1Mo2	2.454(2)
	1P2	2.555(2)		1P1	2.262(2)		1Mo3	2.471(2)
	1P3	2.568(2)		1Ni2	2.573(1)		1Mo4	2.508(2)
	1Ni2	2.607(1)		1Ni3	2.600(1)		1Mo3	2.575(2)
	1Ni4	2.680(1).		1Ni4	2.621(1)		1Mo1	2.580(2)
	1Ni2	2.719(1).		1Ni1	2.627(1)		1Mo5	2.610(2)
	1Ni4	2.736(1)		1Ni4	2.656(1)		1Ni1	2.982(2)
	1Mo5	2.864(1)		1Mo1	2.659(1)			
	1Mo2	2.885(1)		1Mo3	2.690(1)	P2–	1Ni4	2.209(2)
	1Mo1	2.992(1)		1Mo4	2.744(1)		1Ni1	2.228(2)
	1Mo3	2.972(1)		1Mo4	2.746(1)		1Mo1	2.423(2)
				1Ni2	2.757(1)		1Mo4	2.519(2)
Mo3–	1P3	2.427(2)		1P1	2.982(2)		1Mo4	2.541(2)
	1P1	2.471(2)		1P3	3.019(2)		1Mo2	2.548(2)
	1P2	2.555(2)					1Mo2	2.555(2)
	1P1	2.575(2)	Ni2–	1P1	2.221(2)		1Mo3	2.555(2)
	1Ni3	2.668(1)		1P3	2.260(2)		1Mo5	2.624(2)
	1Ni4	2.673(1)		1Ni1	2.573(1)		1Ni2	3.082(2)
	1Ni1	2.690(1)		1Ni3	2.6053(8)			
	1Ni4	2.759(1)		1Mo2	2.607(1)	P3–	1Ni4	2.197(2)
	1Mo5	2.819(1)		1Mo4	2.612(1)		1Ni3	2.255(2)
	1Mo3	2.826(1)		1Ni2	2.664(1)		1Ni2	2.260(2)
	1Mo1	2.952(1)		1Ni4	2.672(1)		1Mo3	2.427(2)
	1Mo2	2.972(1)		1Mo4	2.708(1)		1Mo5	2.536(2)
	1Ni2	2.984(1)		1Mo2	2.719(1)		1Mo1	2.541(2)
	1Mo2	3.262(1)		1Ni1	2.757(1)		1Mo4	2.543(2)
				1Mo3	2.984(1)		1Mo1	2.547(2)
Mo4–	1P1	2.508(2)		1P2	3.082(2)		1Mo2	2.568(2)
	1P2	2.519(2)					1Ni1	3.019(2)
	1P2	2.541(2)	Ni3–	2P3	2.255(2)			
	1P3	2.543(2)		2Ni1	2.600(1)			
	1Ni2	2.612(1)		2Ni2	2.605(1)			
	1Ni3	2.693(1)		2Mo3	2.668(1)			
	1Ni2	2.708(1)		2Mo4	2.693(1)			
	1Ni1	2.744(1)		2Mo1	2.920(1)			

Mo atoms (Mo1 and Mo2) in the (24f) and (24g) positions, respectively, 32 Ni atoms (Ni1 and Ni2) in two (16e) positions, and 16 P atoms (P1) in the (16d) position of the space group. At this stage, a difference Fourier synthesis showed a peak at the origin of the unit cell, corresponding to the (4a) position. Subsequent refinement cycles including thermal factors proceeded smoothly in order to attribute this peak to a phosphorus atom (P2) but with an occupancy factor $\tau = 0.67(1)$. The final difference Fourier map showed no residual peaks larger than $1.6\,e^-/Å^3$. The final formula of this ternary phosphide is therefore $Mo_3Ni_2P_{1.18}$, which corresponds to a quite correct agreement between the refined empirical formula (atomic percentage Mo:Ni:P = 48.50:32.40:19.10) and the nominal overall composition of the bulk sample (49.80:33.70:16.50). The small difference in phosphorus content can be probably attributed to the relative fluctuation of the P2 occupancy factor between bulk and single-crystal samples. Atomic positional and thermal coordinates are listed in Table 5 and selected interatomic distances are given in Table 6.

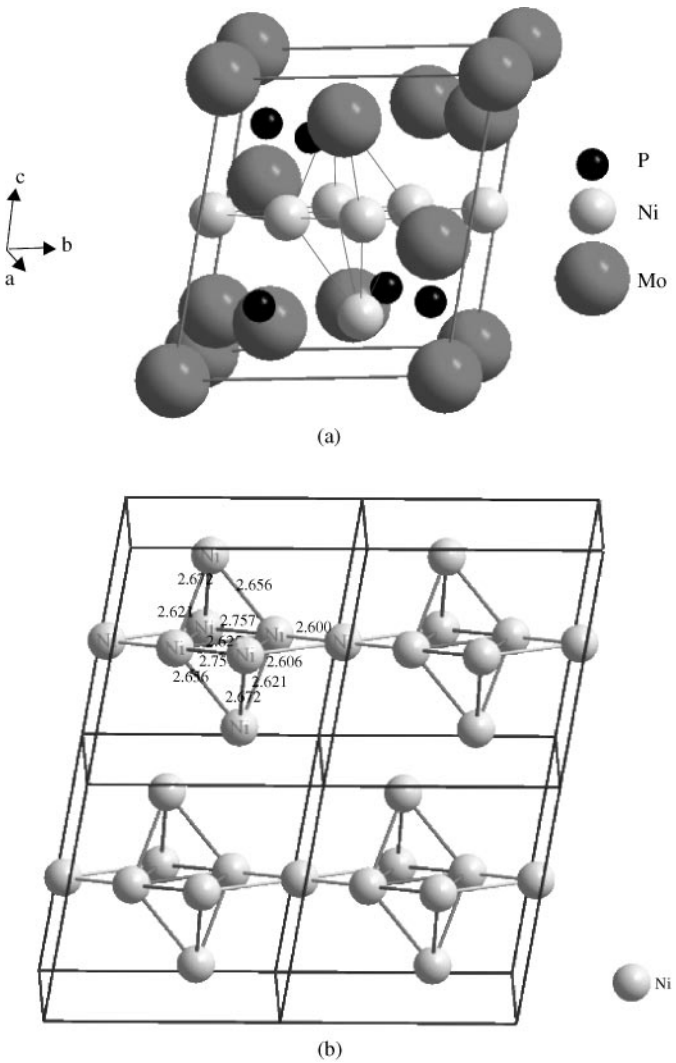

FIG. 3. Crystal structure of $Mo_{8.58}Ni_{7.42}P_6$: (a) 3D representation. Note that the atom at the origin is a pseudo-atom formed by 58.2(6) at.% Mo and 41.8(6) at.% Ni. (b) Chain-like arrangement of nickel atoms along the [010] direction.

TABLE 5
Atomic Positional and Thermal Coordinates for $Mo_3Ni_2P_{1.18}$

Atom	Position	x	y	z	[a]$B_{eq.}$ (Å^2)
Mo1	24(f)	0.19448(7)	0	0	0.43(1)
Mo2	24(g)	$\frac{1}{4}$	$\frac{1}{4}$	0.44468(8)	0.50(1)
Ni1	16(e)	0.16826(8)	x	$-x$	0.49(1)
Ni2	16(e)	0.08090(7)	x	$\frac{1}{2}-x$	0.58(1)
P1	16(e)	0.1229(2)	x	$\frac{1}{2}+x$	0.38(2)
[b]P2	4(a)	0	0	0	0.72(13)

[a]$B_{eq} = \frac{1}{3}[B_{11}\, a^{*2}\, a^2 + \ldots 2B_{23}\, b^*\, c^*\, b\, c \cos(\alpha)]$.
[b]Occupancy factor: $\tau = 0.67(1)$.

Of course, refinement of the crystal structure has been checked in the centrosymmetric space group $Fd\bar{3}m$ and results in the same formula $Mo_3Ni_2P_{1.18}$ with nearly equivalent reliability factors ($R = 0.037$, $R_w = 0.043$). Atomic parameters, which have been transformed from standard choice of the unit cell origin of the $Fd\bar{3}m$ space group to show similarity in the results, are as follows: 48 Mo atoms in the (48f) position ($x = 0.19460(4)$), 32 Ni atoms in the (32e) position ($x = 0.08121(5)$), 16 phosphorus atoms (P1) in the (16d), and about three P2 atoms in the (8a) position (occupancy factor $\tau = 0.33(1)$). Moreover, the equivalent isotropic thermal factors and the interatomic distances are similar to those of the $F\bar{4}3m$ space group (in the limits of standard deviations). However, the structure determination with space group $Fd\bar{3}m$ was not retained for two main reasons: first of all, the use of the centrosymmetric space group omits several weak reflections that do not satisfy the extra condition ($k + l = 4n$) on $0kl$ reflections (id. for $h0l$ and $hk0$). These weak reflections are present in the final data file at the end of the refinement in the noncentrosymmetric space group $F\bar{4}3m$. In addition, the occupancy factor for the phosphorus atoms P2 in the (8a) position ($Fd\bar{3}m$ space group) is $\tau = 0.33(1)$, which corresponds to $\tau = 0.67(1)$ for the same atoms in the (4a) position ($F\bar{4}3m$ space group). When considering the Mo–P2 distance of 2.11 Å, it seems that this distance is in better agreement with an occupancy factor of 67% instead of 33% for P2 atoms when regarding the phosphorus covalent radius. Moreover, that means that the P2 atoms occupy half of the $[Mo_6]$ octahedra in the noncentrosymmetric space group while the second half is empty (see below). In case of the centrosymmetric space group, all the $[Mo_6]$ octahedra should be partially occupied by P2 atoms at 33%. From our point of view, this second possibility seems to be less suitable. Therefore, according to these comments, we have chosen to describe the structure $Mo_3Ni_2P_{1.18}$ in the noncentrosymmetric space group $F\bar{4}3m$.

TABLE 6
Main Interatomic Distances (Å) of $Mo_3Ni_2P_{1.18}$ (< 3 Å)

Mo1–	1P2	2.109(2)	Ni1–	3P1	2.369(2)	P1–	3Ni2	2.302(2)
	2Ni1	2.596(2)		3Ni1	2.508(2)		3Ni1	2.369(2)
	2Ni2	2.734(2)		3Mo1	2.596(2)		3Mo1	2.734(2)
	2P1	2.734(2)		3Mo2	2.730(2)		3Mo2	2.745(2)
	4Mo2	2.842(2)						
	4Mo1	2.983(2)						
			Ni2–	3P1	2.302(2)	P2–	6Mo1	2.109(2)
Mo2–	2Ni2	2.609(2)		3Ni2	2.482(2)			
	2Ni1	2.730(2)		3Mo2	2.609(2)			
	2P1	2.745(2)		3Mo1	2.734(2)			
	4Mo1	2.842(2)						
	4Mo2	2.986(2)						

The crystal structure, shown in Fig. 4, is similar to that of Mn_3Ni_2Si, which is a superstructure of the $NiTi_2$ type (17, 18). The small difference between the silicide and the phosphide in nonmetal content can be easily explained by the covalent radius of silicon (1.17 Å) being larger than that of phosphorus (1.10 Å) (19). Numerous other examples of such a situation can be found in the literature on phosphide and silicide chemistry (20, 21). In agreement with the metal-to-nonmetal ratio being equal to 4.24, the structure of $Mo_3Ni_2P_{1.18}$ exhibits numerous metal-metal bonds (Ni–Ni, Mo–Ni, and Mo–Mo) in contrast to the Mo–P and Ni–P ones. Indeed, the metal atoms are connected to only 2 or 3 P atoms while 12 or 6 metal atoms surround the P1 and P2 atoms, respectively. The main feature of the structure results from the arrangement of Mo atoms, which generate $[Mo_6]$ octahedra in a diamond-like network, with intra Mo–Mo distances of 2.98 Å. Half of the octahedra, which are built by Mo2 atoms, are empty while the second half formed by Mo1 atoms are occupied by phosphorus atoms P2, in partial occupancy ($\tau = 0.67$). These occupied octahedra are displayed in an *fcc* array. However, it is worth noting that the $[Mo_6]$ octahedra cannot be really considered as metal clusters since they are connected through strong Mo–Mo (4×2.84 Å) and Ni–Mo (2×2.596, 2×2.734 Å) interactions. Nevertheless, for a better understanding of the structure, the description by means of $[Mo_6]$ octahedra is evident (Fig. 4). The peculiar disposition of the P2 atom at the center of a $[Mo_6]$ octahedron with relatively short Mo1–P2 distances of 2.11 Å, which can now be rationalized by the partial occupancy (67%) of phosphorus, suggested nevertheless some questions concerning structure refinement. Indeed, this distance was compatible with Mo–O bonding, compared with the sum of metallic and covalent radii of molybdenum (1.39 Å) and oxygen (0.73 Å) (19, 22). Moreover, the recent discovery of an uranium copper oxyphosphide (23) led us to consider the possibility of oxygen atoms, in the (4a) position of space group $F\bar{4}3m$, owing to a possible oxidation of the samples during high-temperature synthesis. Neither structure refinement with oxygen (negative isotropic thermal parameter)

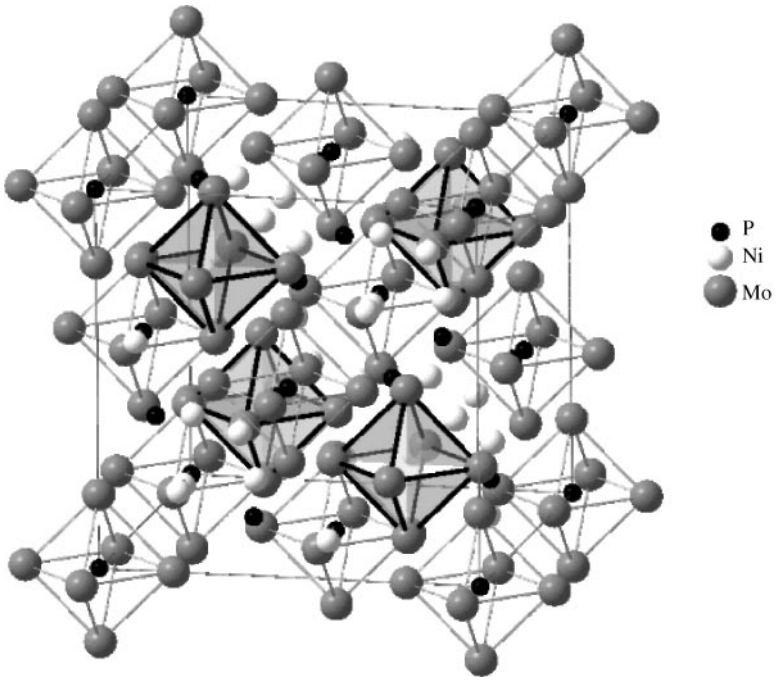

FIG. 4. Three-dimensional representation of the crystal structure of $Mo_3Ni_2P_{1.18}$: Filled and empty [Mo_6] octahedra are emphasized.

TABLE 7
Crystal Data, Intensity Collection, and Refinement for $Mo_{2.675}Ni_{0.325}P$

Empirical formula	$Mo_{2.675}Ni_{0.325}P$
Formula weight (g.mol^{-1})	302.20
Crystal system	tetragonal
Space group	$I\bar{4}$
a (Å)	9.733(1)
c (Å)	4.7805(7)
V (Å^3)	452.9(2)
Z; calculated density (g.cm^{-3})	8; 9.002(3)
Crystal size (mm^3)	$0.035 \times 0.035 \times 0.15$
Linear absorption coefficient (mm^{-1})	17.16
Refinement limits	
θ (°)	1–40
h, k, l	$0 < h < 17$; $-11 < k < 12$; $-5 < l < 8$
Reflections collected	996
Independent reflections (R_{int})	949 (0.065)
Reflections in refinement ($I > 4\sigma(I)$)	908
Variable parameters	39
Absorption correction (T_{min}, T_{max})	0.263, 0.611
Refinement	F
R	0.036
R_w(unit weigh. scheme)	0.047
Extinction coefficient	$63(6) \times 10^{-3}$
Scale factor	0.353(1)
Goodness-of-fit	1.20
Largest diff. peak and hole (e$^-$/Å^3)	2.6/ − 2.0

nor electron microprobe analysis (EDS and WDS measure ments) concluded to the presence of oxygen in this phase. The crystal structure is really that of the new ternary phosphide $Mo_3Ni_2P_{1.18}$.

3. *$Mo_{2.675}Ni_{0.325}P$.* A single crystal was picked from a molten sample of nominal composition Mo_2NiP. The symmetry was found to be tetragonal, with unit cell parameters ($a = 9.733$ Å, $c = 4.781$ Å) close to those of binary Mo_3P ($a = 9.794$ Å, $c = 4.827$ Å) (24). Assuming that this ternary phase was the Ni-rich limit of the substitution solid solution $Mo_{3-x}Ni_xP$ ($x \sim 0.35$), the crystal structure was solved first by taking into account the atomic parameters of Mo_3P. Unfortunately, refinement attempts in the space group $I\bar{4}2m$ were unsuccessful ($R = 0.084$, $R_w = 0.116$). The reliability factors were improved when the structure

TABLE 8
Atomic Positional and Thermal Coordinates for $Mo_{2.675}Ni_{0.325}P$

Atom	Position	x	y	z	$^aB_{eq.}$ (Å^2)
Mo1	8(g)	0.14527(5)	0.99354(5)	0.2478(1)	0.667(9)
Mo2	8(g)	0.40982(5)	0.90388(5)	0.4833(1)	0.572(9)
^{b}Mo3	8(g)	0.30351(6)	0.79132(6)	0.9855(1)	0.84(2)
P	8(g)	0.2099(2)	0.9894(6)	0.7473(4)	0.90(3)

$^aB_{eq} = 1/3[B_{11}\, a^{*2}\, a^2 + \ldots 2B_{23}\, b^*\, c^*\, b\, c \cos(\alpha)]$.
^{b}A mixed Mo/Ni position: 67.5(1.2) at.% Mo and 32.5(1.2) at.% Ni.

TABLE 9
Main Interatomic Distances (Å) of $Mo_{2.675}Ni_{0.325}P$ (< 3.30 Å)

Mo1–	1P	2.470(2)	Mo3–	1P	2.418(2)
	1P	2.474(2)		1P	2.435(2)
	1P	2.481(2)		2Mo3	2.729(1)
	1P	2.494(2)		1Mo1	2.747(1)
	1Mo3	2.747(1)		1Mo1	2.796(1)
	1Mo3	2.796(1)		1Mo2	2.814(1)
	1Mo1	2.831(1)		1Mo2	2.817(1)
	1Mo2	2.905(1)		1Mo2	2.835(1)
	1Mo2	2.943(1)		1P	3.008(2)
	1Mo3	3.038(1)		1Mo1	3.038(1)
	2Mo1	3.101(1)		1Mo2	3.072(1)
	2Mo1	3.134(1)		1Mo2	3.076(1)
	1Mo3	3.275(1)		1Mo1	3.275(1)
Mo2–	1P	2.464(2)	P–	1Mo3	2.418(2)
	1P	2.487(2)		1Mo3	2.435(2)
	1Mo2	2.565(1)		1Mo2	2.464(2)
	1Mo3	2.814(1)		1Mo1	2.470(2)
	1Mo3	2.817(1)		1Mo1	2.474(2)
	1Mo3	2.835(1)		1Mo1	2.481(2)
	2Mo2	2.875(1)		1Mo2	2.487(2)
	1Mo1	2.905(1)		1Mo1	2.494(2)
	1Mo1	2.943(1)		1Mo3	3.008(2)
	1Mo3	3.072(1)			
	1Mo3	3.076(1)			
	2Mo2	3.129(1)			

refinement was solved in space group $I\bar{4}$ (Table 7). The application of direct methods gave four independent atomic positions (8g) occupied by Mo1, Mo2, and P atoms. After refinement with thermal parameters, a mixed Mo/Ni position (67.5 at.% Mo, 32.5 at.% Ni) was allowed on the fourth position. The residual values R and R_w (0.036 and 0.047, respectively) were obtained for 39 variable parameters and 908 structure factors with $I > 4\sigma$ (I). A final difference Fourier synthesis did not reveal any significant electron density peaks. The final formula is therefore $Mo_{2.675}Ni_{0.325}P$ leading to atomic percentages Mo:Ni:P = 66.90:8.10:25.00, not far from those deduced from EPMA: 66.30:7.85:25.85. Atomic positional and thermal coordinates are listed in Table 8 and selected interatomic distances are given in Table 9.

One can suppose that the coordination polyhedra for metal atoms are the same for the binary and the ternary phases. The Mo1 and Mo2 atoms effectively maintain in both structures the same coordination number of CN = 15 and 14, respectively (24). Nevertheless, the mixed (Mo, Ni)3 atom in $Mo_{2.675}Ni_{0.325}P$ exhibits a coordination number of CN = 14 (3 P and 11 metal atoms) instead of CN = 15 (4 P and 11 Mo) for Mo3 in the binary phase.

The structural results do not strengthen the hypothesis of a continuous solid solution between Mo_3P and $Mo_{2.675}Ni_{0.325}P$, since the space groups differ from each other ($I\bar{4}2m$ for the binary, $I\bar{4}$ for the ternary). Unfortunately, no evident solution can be deduced from the examination of their theoretical X-ray diffraction patterns (Fig. 5). Therefore, powder samples of the solid solution that have been studied do not make it possible up to now to come to a definite conclusion. Consequently, it appears absolutely necessary to check out the space group of Mo_3P with more details because the structure of the binary was solved 30 years ago from X-ray powder or single-crystal data using photographic methods (24, 25).

CONCLUSION

The reinvestigation of the Mo–Ni–P system at high temperature (1350°C) has shown the existence of numerous ternary phases. Among them, two correspond to Ni-rich limits of substitution solid solutions: MoNiP of Fe_2P type and $Mo_{2.675}Ni_{0.325}P$, a derivative of Mo_3P type, while the other phases appear as ternary compounds. In addition to the crystal structures previously reported, three new structures were solved on single crystals: triclinic $Mo_{8.58}Ni_{7.42}P_6$ ($P\bar{1}$), cubic $Mo_3Ni_2P_{1.18}$ ($F\bar{4}3m$), and tetragonal $Mo_{2.675}Ni_{0.325}P$ ($I\bar{4}$). Unfortunately, the structure determination of two phosphides $Mo_9Ni_6P_5$ and $MoNi_2P$ has been unsuccessful so far, owing to the absence of single crystals or pure powder samples. Combining X-ray diffraction together with scanning electron microscopy and electron probe microanalysis enabled us to confirm overall the results previously reported at 850°C, with the exception of two new phases, $Mo_3Ni_2P_{1.18}$ and $Mo_{2.675}Ni_{0.325}P$, which were obtained in molten samples at 1350°C. In order to conclude definitively on the Mo–Ni–P system, additional studies should be done to characterize structurally the last two phases $Mo_9Ni_6P_5$ and $MoNi_2P$.

The X-ray structures of $Mo_{8.58}Ni_{7.42}P_6$, $Mo_3Ni_2P_{1.18}$, and $Mo_{2.675}Ni_{0.325}P$ on single crystals exhibit numerous and strong metal–metal bonds in relation with metal-to-nonmetal ratios higher than 2.5. The phosphorus coordination number for molybdenum and nickel atoms is very small such that metal arrangements, for example, [Ni_4] tetrahedra and [Mo_6] octahedra in the structures of $Mo_{8.58}Ni_{7.42}P_6$ and $Mo_3Ni_2P_{1.18}$, respectively, can be viewed. Moreover, it is important to note that half of the [Mo_6] octahedra in $Mo_3Ni_2P_{1.18}$ are centered by phosphorus atoms in partial occupancy (67 at.%).

Attempts to measure the intrinsic physical properties of the molybdenum nickel phosphides were difficult owing to the small size of the single crystals. Some preliminary experiments on sintered powder samples were carried out to define the magnetic behavior. As expected, a temperature-independent paramagnetism (TIP) of Pauli type was found, in agreement with the metallic character of these phases. Finally, superconductivity in the binary Mo_3P phase ($T_c = 4.2$ K)(26) is encouraging for measuring precisely the electrical properties of some of these molybdenum nickel phosphides, synthesized as pure samples.

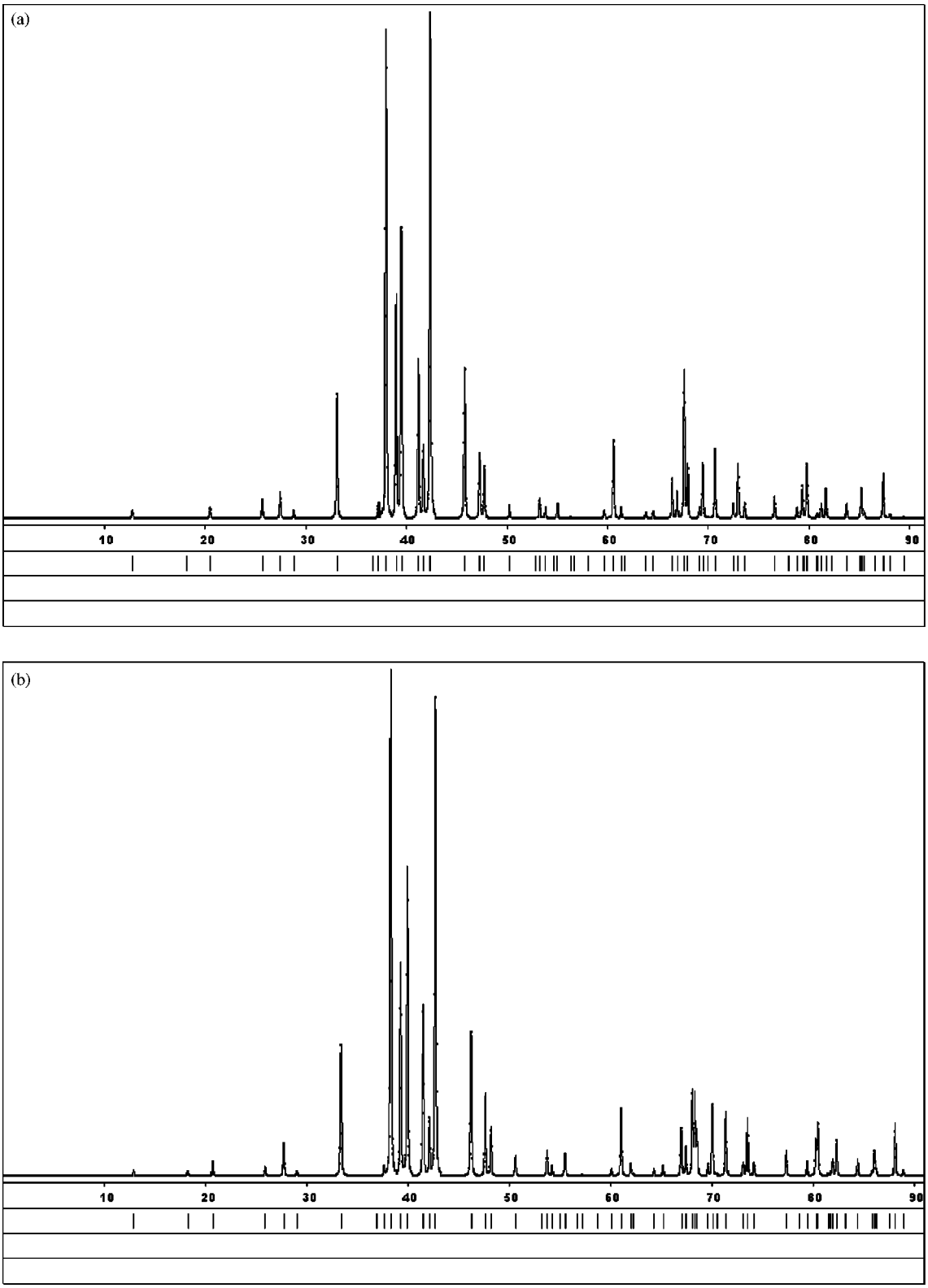

FIG. 5. Theoretical X-ray diffraction patterns of: (a) Mo_3P and (b) $Mo_{2.675}Ni_{0.325}P$.

ACKNOWLEDGMENTS

One of the authors (S.V.O) is grateful to the French Ministry (MAE-MENRT) for a financial support through a high-level research grant. The authors also thank T. Roisnel (Centre de Diffractométrie, Université de Rennes 1) for X-ray intensity data collection and J.-C. Jegaden and J. Le Lannic (CMEBA, Université Rennes 1) and M. Bohn (IFREMER, Brest) for their assistance in the SEM and EPMA studies.

REFERENCES

1. R. Guérin and M. Sergent, *C.R. Acad. Sc. Paris* **281,** 777 (1975).
2. R. Guérin and M. Sergent, *Mater. Res. Bull.* **12,** 381 (1977).
3. R. Guérin and M. Sergent, *J. Solid State Chem.* **18,** 317 (1976).
4. R. Guérin and M. Sergent, *Acta Crystallogr. Sect. B* **33,** 2820 (1977).
5. S. V. Oryshchyn, Yu.B. Kuz'ma, and N. G. Markiv, *Dop. Akad. Nauk Ukr. Rsr.* **43,** 80 (1981).
6. S. V. Oryshchyn and Yu.B. Kuz'ma, *Sov. Phys. Kristallogr.* **25,** 612 (1980).
7. COLLECT: KappaCCD software, Nonius BV, Delft, The Netherlands, 1998.
8. Z. Otwinowski and W. Minor, *in* "Methods in Enzymology" (C. W. Carter, Jr., and R. M. Sweet, Eds), Vol. 276. Academic Press, New York, 1997.
9. R. H. Blessing, *Acta Crystallogr. Sect. A* **51,** 33 (1995).
10. L. G. Aksel'rud, Yu. N. Grin, V. K. Pecharsky, and P. Yu. Zavalij, "CSD97—Universal program package for single crystal and powder data treatment," Version N7, 1997.
11. G. Cascarano, A. Altomare, C. Giacovazzo, A. Guagliardi, A. G. G. Moliterni, D. Siliqi, M. C. Burla, G. Polidori, and M. Camalli, *Acta Crystallogr. Sect. A* **52,** C-79 (1996).
12. V. Petricek and M. Dusek. "JANA2000: Crystallographic Computing System for Ordinary and Modulated Structures." Institute of Physics, ASCR, Praha, Czech Republic.
13. K. Brandenburg, "Diamond," Version 2.0 (1998).
14. S. Rundqvist and F. Jellinek, *Acta Chem. Scand.* **13,** 425 (1959).
15. M. V. Dewalsky and W. Jeitschko, *Acta Chem. Scand.* **45,** 828 (1991).
16. F. Charki, S. Députier, P. Bénard-Rocherullé, R. Guérin, M. Bouayed, A. LeBeuze, and J. Y. Saillard, *Solid State Sci.* **1,** 607 (1999).
17. E. I. Gladyshevskii, Yu.B. Kuz'ma, and P. I. Kripyakevich, *J. Struct. Chem.* **4,** 343 (1963).
18. M. H. Mueller and H. W. Knott, *Trans Met. Soc. AIME* **227,** 674 (1963).
19. L. Pauling, *in* "Nature of the Chemical Bond," 3rd ed. Cornell Univ. Press, Ithaca, NY, 1960.
20. J. Y. Pivan and R. Guérin, *J. Solid State Chem.* **135,** 218 (1998).
21. C. Le Sénéchal, V. Babizhets'ky, S. Députier, J. Y. Pivan, and R. Guérin, *J. Solid State Chem.* **144,** 277 (1999).
22. F. Laves, "Theory of Alloy Phases." Am. Soc. Metals, Cleveland, OH, 1956.
23. D. Kaczorowski, M. Potel, and H. Noël, *J. Solid State Chem.* **112,** 228 (1994).
24. B. Sellberg and S. Rundqvist, *Acta Chem. Scand.* **19,** 760 (1965).
25. S. Rundqvist, *Nature* **211,** 847 (1966).
26. B. T. Matthias, E. Corenzwitt, and C. E. Miller, *Phys. Rev.* **93,** 1415 (1954).